Influence of processing parameters and their acceptance criteria in the plasma spraying of WC-Co -based A.P.S coatings on corrosion, Physical, thermo physical, chemical, and mechanical properties in the Aerospace and Defense Industries

Khaled Fared Ahmed[2] *

1*Assistant Professor, Buraydah Private Colleges. - Al Qasim Arabic Kingdom of Saudi Arabia1-Abstract (khalidfared330@yahoo.com)

1- Abstract

Material performance in many industrial applications is strongly affected by the behavior of the surfaces. For example, corrosion response reactivity with environments, wear characteristics, and thermal properties are all critically dependent on surface character. The advantage of coating technology, in general is that it marries two dissimilar materials to improve the performance of the whole.

There are two approaches to improve the carbide coating in plasma spraying. One method is the optimization of the spray parameters to improve the adhesion properties and decrease the solidification rate. The other method is using high W-carbide content powder (88% W-carbide + 12% Co).Our objective is not only to spray high content tungsten carbide (WC – 12wt% Co), but also to get the best optimum spray parameters, by studying the effect of these parameters in microstructure, adhesion, reaction layer, micro-hardness, corrosion and pore formation.

Key words: Thermal spray, A.P.S, spray parameters, thermo physical properties, WC-Co coatings, amorphous microcrystalline, and metastable phase.

2-Introduction

Aim and Scope of the Present Work.

Plasma is quasi-neutral multi particles system which characterized by gaseous or fluid mixtures. It consists of electrons, positively changed ions and neutral gas, atoms, molecules or radicals. Mono-atomic gases require only to be ionized in order to enter the plasma state, while bimolecular gases must be first

dissociated before ionization, thus need larger energy to enter plasma state. Small quantities of hydrogen (or helium) added as a secondary gas to argon lead to increase of both plasma enthalpy and heat transfer rates from the plasma to the powder particles. There are many spray parameters that affects the properties of the sprayed plasma coating, the most common control parameters are: Chemical compositions, phase structure and crystal size of the powder input, substrate temperature, plasma gas, plasma torch, powder feeder (.e.g. grain size chemical and phase composition, shape, internal porosity (correlated with apparent density) and flow-ability), spray angle, and finally spray distance.The objective of this study is to improve the temperature wear, and corrosion resistant, properties of steel alloys materials via plasma using metal carbide or ceramic powder. Recently, there are many surface modification processes to steel by the evolution of effective lubrication with higher performance to keep the lubricating systems running reliably and to avoid bearing and other component failures (1), and plasma thermal spray coatings process (2-6).

Plasma spraying is the most versatile of the coating technologies. It may serve for "metalizing" all sorts of articles and has great advantages over the known galvanizing process in cases where it can be used to coat electrically non-conductive surfaces with metal. Spray materials must be melted and sprayed without decomposition or excessive vaporization in plasma flame through the optimum spray parameters. In plasma spray process, the spray material in the form of powder is rapidly brought to molten or near molten state by the plasma flame and then accelerated by a gas stream to impact a suitably prepared substrate. Upon impact, the molten metal droplets are rapidly flattened and solidify to form their splats. Microstructure and physical properties of sprayed coatings are linked to dynamic properties of molten particles impinging on a substrate.Plasma spraying of ceramic or carbide coating is a prime candidate for the surface modification of steel alloys for anti-wear corrosion, erosion and thermal resistance. Carbides powder during spraying is not quite easy process because of rapid solidification of flattened particles (7-8).

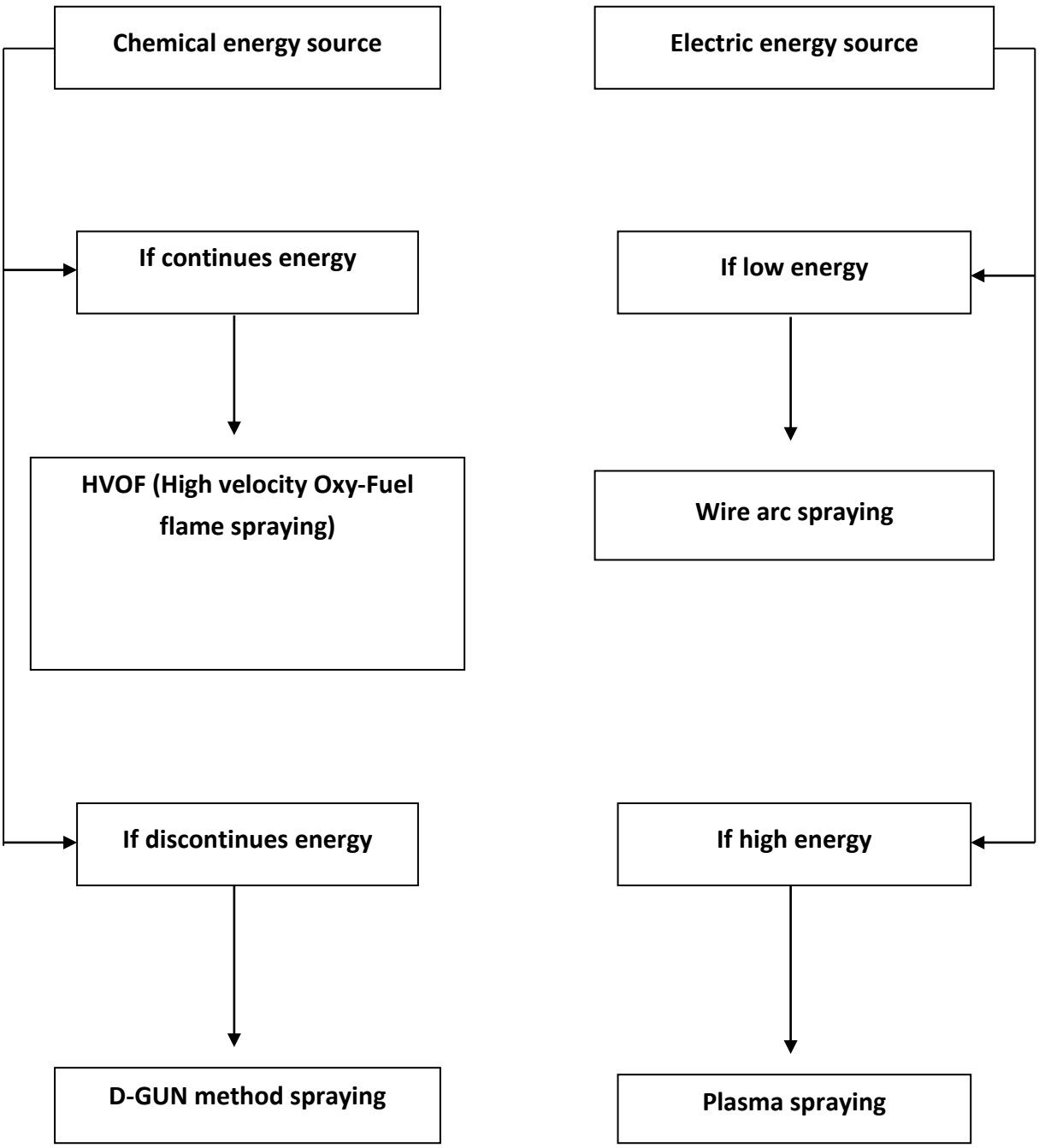
Review

Thermal spraying requires a device used for flame spraying that creates a high temperature flame in which a chemical energy of the combusting gases that power the flame spray torches (9-16). A plasma generator powered by arc or high frequency discharge, whose plasma is supported by streaming gas. In which an electric currents providing energy that power the plasmatron. The following diagram shows the different thermal spraying techniques according to the energy sources (16-23).Air plasma spraying (APS) considered being an effective rapid solidification technique. The process can be referred to as continuous meta-stable materials forming (24, 25). It is being considered for the production of wear- and corrosion-resistant coatings (26, 27). Such high temperatures caused self-annealing of the deposits on the substrate which provides stress relief and re-crystallization and results in enhanced inter-particle bending (28). Plasma is quasi- neutral multi particles system characterized by gaseous or fluid mixtures. It consists of electrons, positively changed ions and Neutral gas, atoms, molecules or radicals (29). Mono-atomic gases require only to be ionized in order to enter the plasma state, while bimolecular gases must be first dissociated before ionization, thus need larger energy to enter plasma state. Small quantities of hydrogen (or helium) added as an auxiliary gas to Argon lead to increase of both plasma enthalpy and heat transfer rates from the plasma to the powder particles (30). The powder particles are injected into the plasma flame by means of carrier gas flow through an injector. There are several ways for injection into the plasma jet. The distribution of particles in the plasma jet and the deposition efficiency are controlled by injection parameters (31, 35). Plasma spray coatings are produced by successive impacts of accelerated particles in a molten state on the substrate or previously deposited layers, the next particle impacting on an already completely solidified one. The conditions of these particles (temperature, velocity and size) and the condition of the substrate (temperature, chemistry, roughness … etc.) determine the particle spreading and solidification. Coating quality obtained during thermal spraying depends greatly on the dynamics of flattening of the molten droplets during their impinging on the substrate surface

(36, 48). Particles with sizes substantially larger than the main do not melt completely to their core and thus do not spread on impact. Thus it is extremely important to utilize spray powders with a narrow particle size distribution with a sufficiently small standard deviation (49).

Flattening of thermally sprayed particles (droplets) develop splats on the substrate and/or on the prior deposited coating layers. The splat formation process is influenced by various parameters as impinging velocity, liquid viscosity, and surface tension of molten droplet, substrate materials and substrate temperature. (50-53).The flattening and cooling begin immediately after droplet impingement and the main cooling is caused by the heat removal from the lower part of the splat adjacent to the substrate. This heat removal depends on the initial temperatures and thermo physical properties of the substrate and splat as well as on the contract thermal resistance at the splat-substrate interfaces (54-55).

Oxidation of coatings during thermal spraying essentially influences their structure and properties (56-70). Corrosion behaviour of different ceramic coatings fabricated by plasma spraying was investigated (71-73), the corrosion resistance was sharply improved due to decreased amount of connected pores in the coatings.



Principle Diagram of the Energy Source Shows the different thermal spraying techniques divided by their principle energy sources.

3-Methods

3.1. Process Description.

A path is pre-ionized for the direct current arc from the cathode to the anode using high frequency (HF) sparking. The direct current arc, energized from the power source ionizes the gas flowing through the torch (ionization = electron excitation). The gas flow drives the arc contact point in the anode nozzle forward and the arc stabilizes. Argon gas is used for arc initiation (easily ionized) and following stabilization, an auxiliary gas is normally added, such as H_2 or N_2 (with two atoms) dissociate at high temperatures before ionizing. Therefore, they exhibit a higher energy (for a certain temperature) than gases such as Ar. or He. (single atoms). The mixture of electrons, ions and neutral gas particles is the plasma i.e. a gas with an extremely high temperature (between 10000 and 30000 k) and heat capacity. The increase in temperature causes the plasma to exit from the anode nozzle with a high velocity. The spray powder is introduced into the hot, fast plasma using an injector and the particles are heated and accelerated. The powder particles become molten and impact on the surface to be coated with a high kinetic energy where they form a laminar coating. Plasma spray coating is produced by successive impacts of accelerated particles in a molten state on the substrate or previously deposited layers, the next particle impacting on an already completely solidified one. The conditions of these particles (temperature, velocity and size) and the conditions of the substrate (temperature, chemistry, roughness, etc.) determine the particle spreading and solidification. The PLASMA-TECHNIK AG standard units are supplied with automatic systems for the basic functions, e.g. start-up and shut-down and monitoring the spray parameters. Figure (1) shows the schematic diagram of the PLASMA-TECHNIK AG M- 1000 apparatus. The use of plasmatex powder, which have to meet extremely high quality standard will result in coating of extremely good quality using PLASMA-TECHNIK AG spraying parameters. In our investigation we use 301 plasmatex powder corresponding to WC-Co powders.

3.2. Selection of plasma gases.

Argon: (Ar.): It is used as primary plasma gas. It is an inert gas and protects the power particles from any damaging atmospheric influences. It should be used with nitrides which tend to dissociate. Hydrogen (H_2): A mixture of pure Ar and H_2 protects against oxidation. The small addition of H_2 increases the plasma voltage (dissociation and ionization) and therefore allows spraying at a higher plasma torch power level which results in a higher plasma gas heat capacity. The purity level of the gases used plasma spraying is given in the following; it must be observed at all times of investigation.

Gas	Purity (%)	Impurities (volume parts per million)
Argon	99.997	$O_2 < 5$, $N_2 < 10$, $H_2O < 5$, $CO_2 < 0.2$
Hydrogen	99.997	$O_2 < 10$, , $H_2O < 20$

3.3 Spraying Materials Investigation.

The chemical composition in (weight %) and powder description of sprayed materials is given in table (1). The characteristics of sprayed and their acceptance criteria for coating is given in tables (2).

The key parameters controlling the thermo-mechanical properties of plasma sprayed (D.C. plasma spraying) are the heat and momentum transfers between the plasma jets and the injected particles. These, beside the particles side and plasma gas nature, depends strongly on the plasma isotherms lengths and diameters which in turn controlled by nozzle. Table (3) shows the different spray parameters of control unit PT-M1000, powder feeder (TWIN 10) and plasma torch F4.

3.4 Substrate Material Investigation.

The substrate of a flat steel alloy sheet with dimensions (40x20x1.2mm) processing includes a polishing step with emery papers followed by cleaning with tap water and acetone as final step. The specimens were preheated from 60-100^{o}C then rinsed with acetone again. To improve the mechanical adhesion of the coatings and induces compressive stresses into the substrate material, the substrate was roughened using automatic adjustable device (robotized). The

chemical composition of the steel alloy substrate material used is listed in table (4) as detected by XRD (X-ray diffraction) (Fig. 2). The quantitative identification of the base material has analysed by using spectrum technique (EDX) analysis, Fig. (3). the optimum parameters of substrate material preparation for applying spray coating is given in table (5).

Table (1): Chemical composition and powder number of sprayed materials used:

Spray powder	Powder no. in		Chemical composition (%)		Kind
	Amdry plasmatex	METCO			
Tungsten carbide	301	71 (VFNS)	WC	Co	Carbide powder
			88	12	

Table (2): Characteristics of sprayed powders and their acceptance criteria for plasma coating

Allowed thick-ness (mm)		Grain size (μm)	Micro hardness ($H.V_3$)	Tensile bond strength (M.Pa.)	Porosity (%)
Min.	Max.				
150	250	5 – 45	700	45	< 5
The un-bounded particle percent is 5%					

Table (3): Spray parameters of control unit, powder feeder and plasma torch for thermal spraying of tungsten carbide materials

(A) Control unit (PT M1000) parameters

Spray powder	Gases	Flow rate (L/min)	Pressure (bar)	Current (Amp)	Voltage (V)
Tungsten carbide	Main gas Ar.	65	2.5	750 ~ 800	~ 60
	Secondary gas (H_2)	4.5	2.5		

(B) Plasma torch (Gun) parameters

Spray powder	Gun type	Injector diameter (mm)	Injector distance (mm)	Injector angle (degree)
Tungsten carbide	F4	1.5	5.5	75 º

(C) Powder feeder (Twin 10) parameters

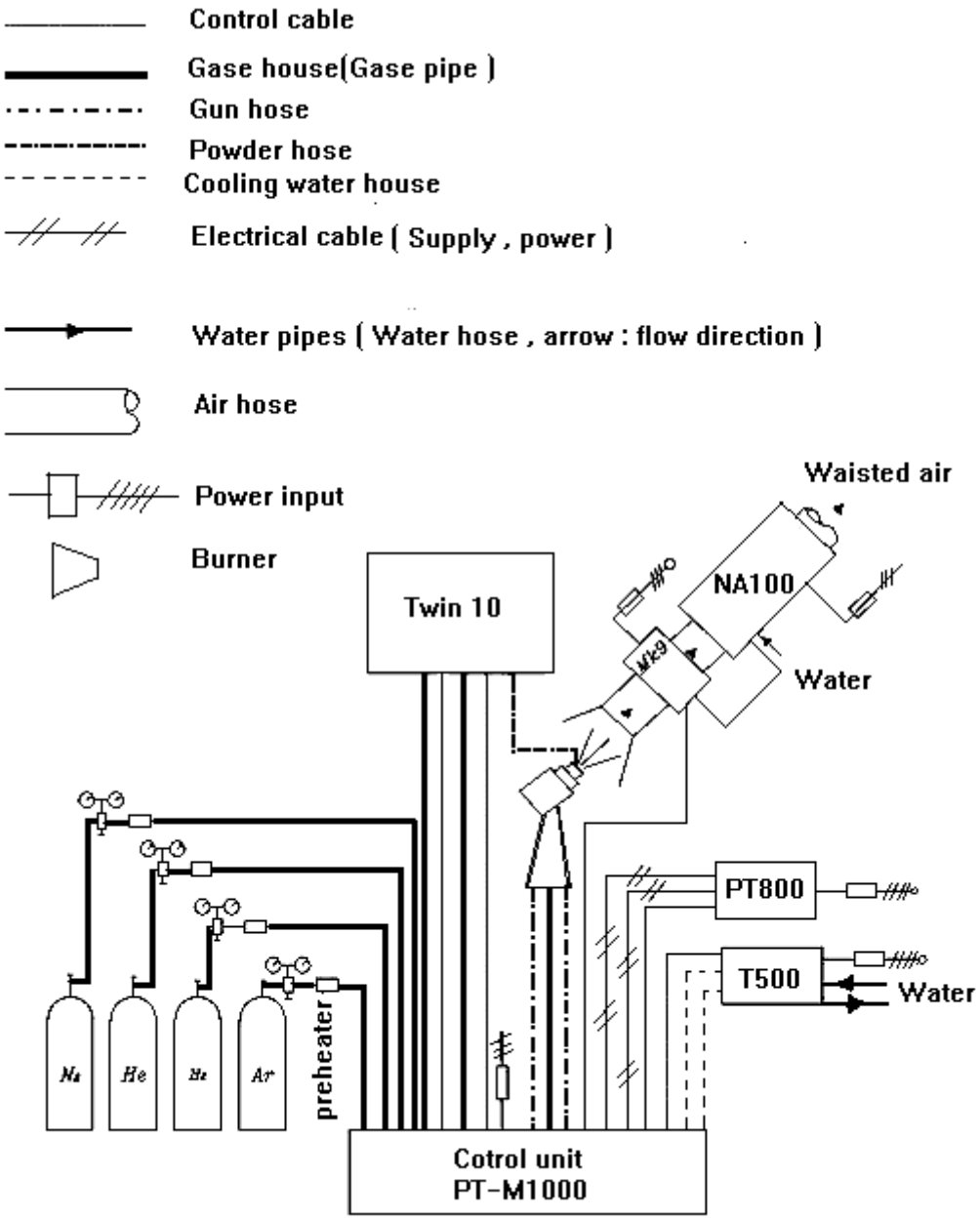
Spray powder	Carrier gas			Spraying distance (mm)	Flow rate (g/min)	Coating thickness (mm)	Cooling
	Type	Pressure (bar)	Flow rate (L/min)				
Tungsten carbide	Ar.	2.5	2.6	125-130	35	150-250	Air

Table (4): Chemical composition in (wt. %) for substrate material

C%	Si %	Mn. %	P %	S %	Cr %	Ni %	Ti %	Fe %
0.08	0.08	2	0.035	0.025	17	9	0.7	Residual

Table (5): Optimum parameters for preparation of substrate material

Grain size (μm)	Pressure (KPa.)	Torch distance (mm)	Surface speed	Angle (degree)	Nozzle diameter (mm)
120 ~ 300	300 ~ 400	150	Manual	75º	10



<u>Fig. (1):</u> Systematic diagram of Plasma Spray M-1000 (plasma-Technik-A G)

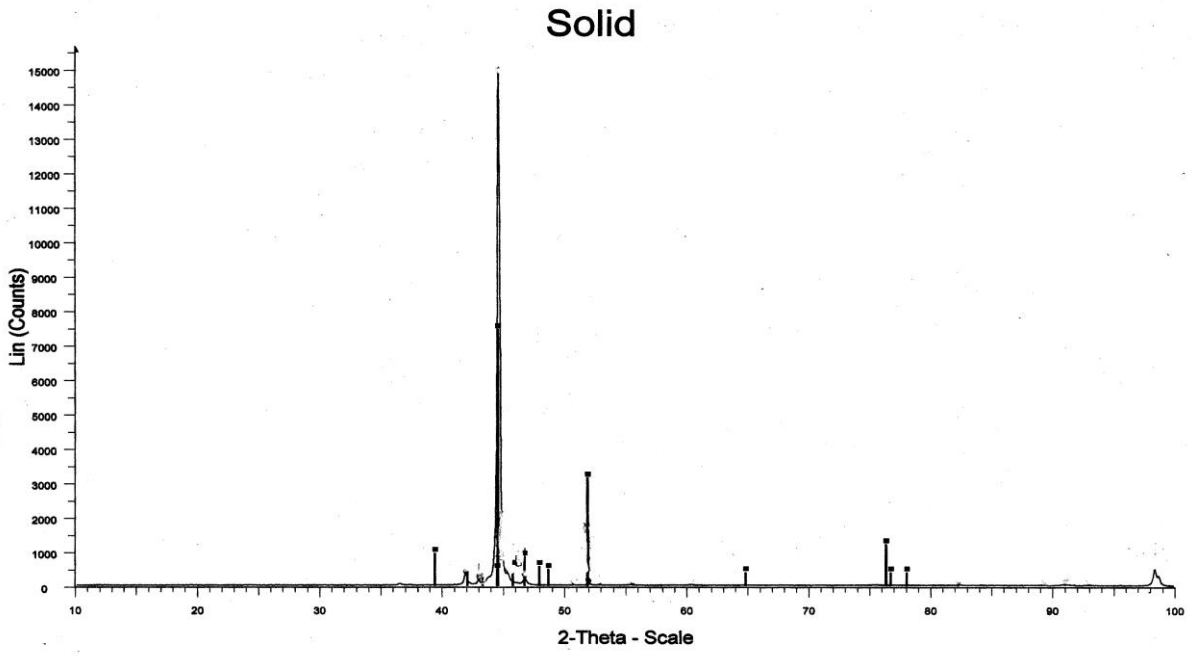


Figure (2): *X-ray diffraction pattern of the base material*

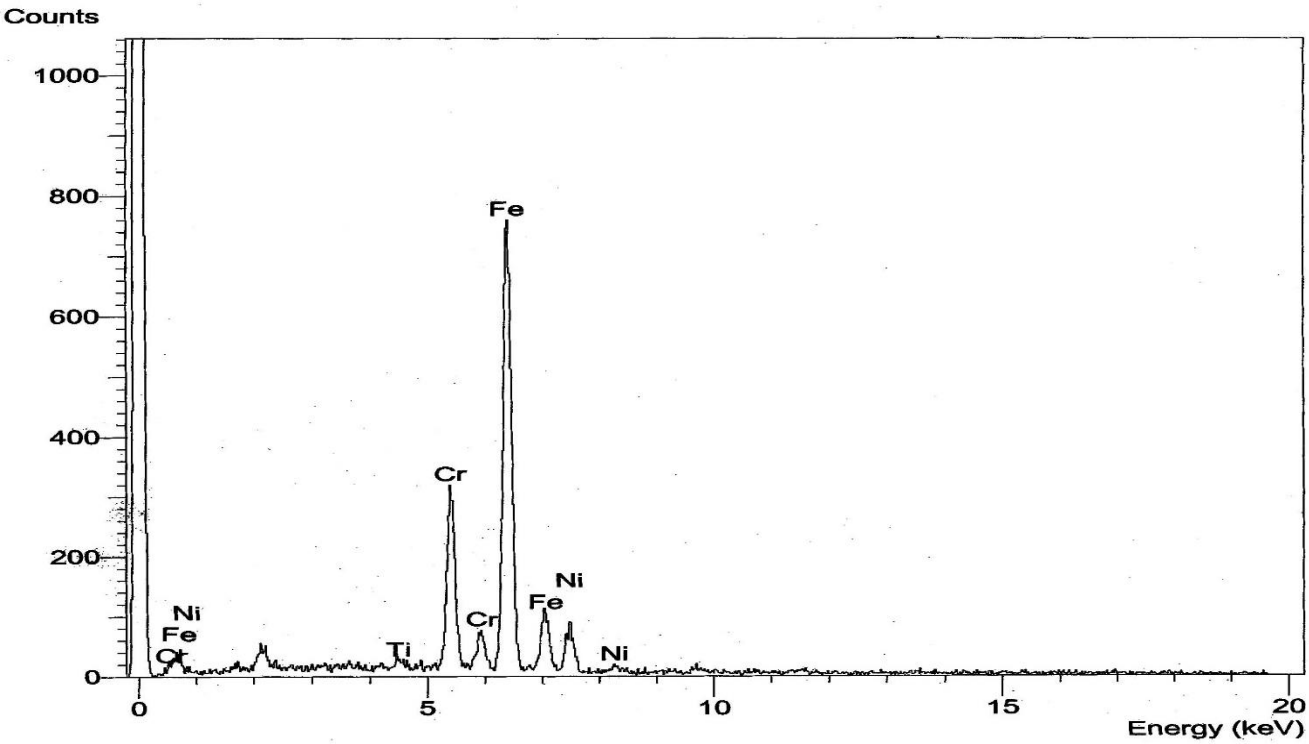


Figure (3): *Electron dispersive X-ray (EDX) spectrometry pattern of the base material*

3.5 Metallographic Investigation.

A sample, on which a deposit has been applied, is cut perpendicular to its coated surface, then encapsulated and polished. Micrographic cross-section is initially, observed overall magnified by 100 or 200 times. Area considered as representative of the sample are re-examined with a magnification of 200-1000. Cross sections were made in the plane perpendicular to the treated surface using an optical microscope with different magnification. The metallographic examinations of the coat have been investigated by using scanning electron microscopic examinations (SEM). The material of a flat sheet metal specimen (low carbon alloy steel) has the following dimensions 40 mm x 20mm x 1.2mm after having coated the specimen thickness surface, make a cross-section perpendicular to the scanning direction. The coating thickness to be applied (measured with a flat anvil micro-meter) is mentioned on the drawing or any additional document, with a 0.12mm minimum.

3.6 Mechanical properties investigation.

The micro-hardness of the treated and untreated surfaces was determined using identical micro-hardness tester using micro-Vickers machine with 30 gm. load for 15 second. The hardness after plasma thermal spraying process at different zones was determined for surface-treated specimens. A specimen without plasma thermal spray coating was used as reference. The Vickers micro-hardness test is used for coatings measurements under load 3N (e.g. HV_3 is the Vickers number for 3N load) describe the micro-hardness of individual lamellae. The commercially available testers flow the normal procedures (e.g. ASTM E-384-73 standard).

Tensile bond strength is measured by using ASTM 633-96 or DIN 50160 standard. Bonding of sprayed coating is measured by using a traction machine. The installation must allow carrying out the test perpendicular to the coated surface, and the load application rate must be constant, between 0.8 and 1.2mm/min^{-1}. Bond strength value or stress to rupture is the ratio between the

rupture load and the bonding surface; this is expressed in migapascale (M.Pa). For coating with a single layer, a thickness required is 150μm to 200μm. Surface preparation conditions for receiving the coating must be identical to those applied on the item. The surface to be glued must be degreased, sand blasted and dusted. Gluing process takes place by use FM1000 epoxy polyamide film glue (American Cyanamid) or equivalent.

3.7 Particle Velocity and Surface Temperature Measurements.

Especially in the field of particle diagnostics, many systems are available to measure particle velocity and surface temperature on-line (74-77). One of the particle measurement systems is the DPV-2000 system made by TECNAR Canada. The DPV-2000 system enables the on-line measurement of surface temperature, velocity and diameter of single particles in a spray plum by the principle of two-wavelength pyrometer (77, 78). In this study, a commercially available DPV-2000 system was used to investigate APS of WC-Co. The investigation centred on the influence of the spray parameters on the particle in-flight properties and the melting behaviour of the power.

3.8 Porosity and pore distribution Measurements.

The thermally sprayed coatings are composed at least two phases: porosity and solid matrix. Very often the solid matrix contains separate phases resulting from rapid solidification and cooling. The normal procedure for coating materials (e.g. American B 328-73) seems to be quite well adapted to test thermal sprayed coatings. Porosity were tested with commercially available mercury intrusion porosity-metre (MIP). The method consists of evacuating the sample and immersing in mercury at low pressure (Whittemore, 1981). The mercury is then pressurized and the series of pressures and corresponding volumes of intruded mercury is determined. This method enables the total porosity and pore distribution to be determined. The porosity influences many mechanical and physical properties of the coatings. Finally, the determination of the porosity in many cases enables the predication of other properties of the

sprayed material. The chemical compositions (wt.%) of the coat have been investigated by using electron dispersive x-ray (EDX) analysis and the phases formed due to thermal spray process have been examined by means of x-ray diffraction (XRD).

3.9 Corrosion Resistance Test.

Electrochemical accelerated corrosion experiments were performed in a conventional three electrode glass cell assembly with the specimen as the working electrode. The specimen is tightened to the outside face of the cell using two screws. Stainless steel rod was used as the counter electrodes while the reference electrode was Ag / Ag Cl. The electrolyte was consisted of 3.5% Na Cl. solution made up from distilled water and reagent grade Na Cl. (Fisher scientific) Experiments were carried out at room temperature. The electrical contact was achieved through thick copper wires soldered to the electrodes.

Linear polarization and potential-dynamic techniques were used to determine the corrosion rate as well as the corrosion behaviour of specimens. These experiments were carried out using AUTOLAP PGSTAT 30 show in fig. (4).

Accelerated corrosion experiments were carried out using; linear polarization technique by subjecting the working electrode to a potential range of 25mv below and above corrosion potential ($E_{corr.}$) at a scan rate of 0.1mv/sec. The corrosion current (I_{corr}) and hence the corrosion rate (CR) can be related to the slope of the potential vs. current plot ($\Delta E/\Delta I$), known as the polarization resistance (R_P) and simply by $I_{corr} = B/ R_P$, where B is a constant. Potential-dynamic polarization tests were conducted by sweeping the potential with scan rate of 1mV/s from -100 mV below E_{corr} into 1000 mv above E_{corr}. This test was performed to study the corrosion behaviour of specimens before and after plasma thermal spray technique.



AUTOLAP PGSTAT 30



Corrosion cell

***Figure (4):** Photograph of AUTOLAP PGSTAT 30 and corrosion cell*

4. Results and Discussion

4.1 Plasma Spray Parameters and Coating Performance.

The effect of plasma spray parameters on coating performance can be illustrated in Tables (6-10), while all other parameter was Kept constant (Table 3). Arc voltage versus H_2-content can be illustrated in figure (5). Metallography/ Image Analysis – photomicrographs of sprayed Tungsten carbide (WC-12 wt. % Co) coatings with different spray parameters are show in figure (6). The deviation of the plasma spray parameters from the optimum condition lead to the fine microstructure of high dense coating become lower in quality i.e. increase of porosity, voids (Pull-out effect), un-melted phase, and de-lamination. The coating/substrate interface of the as- sprayed samples (Plasma spray at optimum condition) is very sharp and distinct with no apparent visual evidence of any metallurgical reaction at this interface. As the secondary plasma gas flow rate increases, the arc voltage increases (it is rises from 27 volts for pure argon to 60 volts when hydrogen content in Ar-H_2 mixture is equal to 7%) the deposition of high dense coating with fine microstructure increases (low porosity). This phenomena lead to increase of the micro-hardness, tensile bonding strength, corrosion resistance and thickness of the sprayed matrix alloy. On decreasing of the H_2-gas flow rate from 4.5 L/min to 3.5 L/min, increasing of the arc current from 750 A to 850 A, decreasing of the arc current from 750 A to 450 A, decreasing of the injector angle from 75º to 35º, wrongly placed of cooling air jets , decreasing of the spraying distance from 13 mm to 75 mm, or increasing of the spraying distance from 130 mm to 200 mm and keeping all other parameters constant lead to change in the mechanical and physical properties of the obtained coating layer. These are due to decreasing of arc voltage from 60 V to 50 V, increase of the pumping effect, decrease in the deposition efficiency, and the number of droplet which impact normally decreases, increase of the substrate temperature or a deviation occurs for the droplet during flight for long distance respectively.

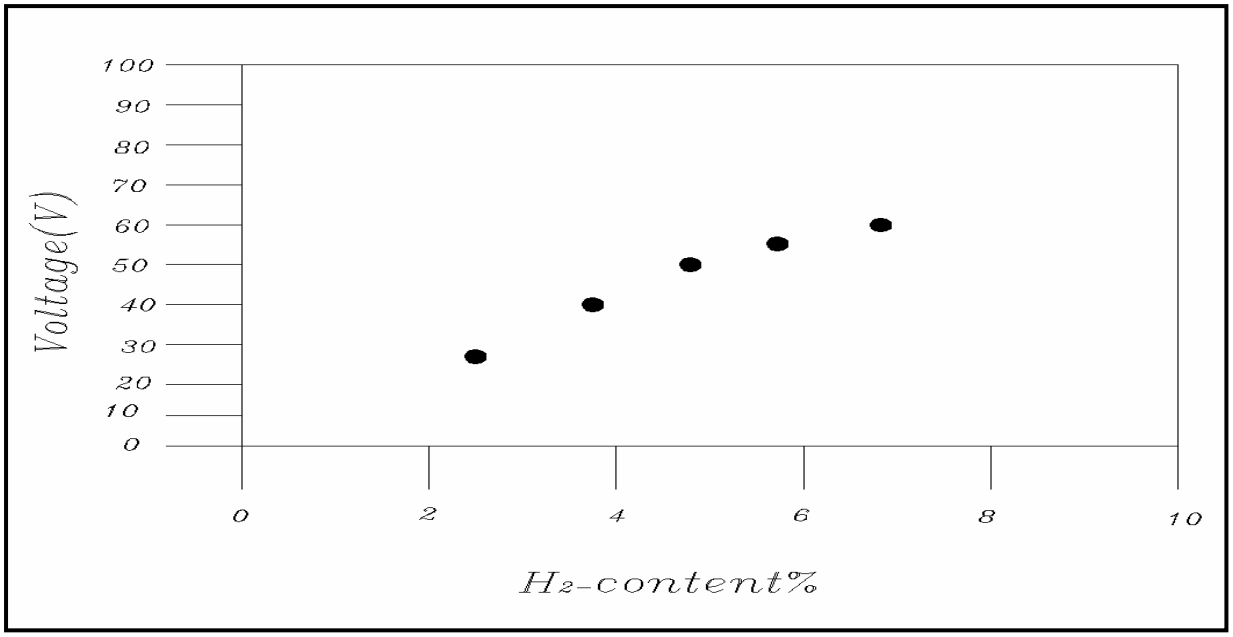


***Figure (5):** Arc Voltage versus H_2-content: Total Flow Rate=70L/min: I=750AF or WC-12Wt% CO Coating*

***Table (6):** Show the effect of the plasma gas on the coating performance at arc current = 750 A, injection angle = 75°, substrate temperature =140 C°, and injection distance = 130mm*

Specimen No.	Plasma gas flow rate (L/min)		H2-content (%)	Arc voltage (v)	Hardness (Hv_3)	Tensile bond strength (M.Pa)	Corrosion rate (mpy	Porosity (%)	Thickness (μm)
	Ar	H_2							
$^{/}S_0$	65	4.5	6.9	60	700	45	$0.12 X10^{-3}$	2	220
$^{/}S_1$	65	3.5	5	50	688	44.3	$4x10^{-3}$	7	160

***Table (7):** Show the effect of the plasma gas on the coating performance at Ar-gas flow rate = 65 L/min, H_2-gas flow rate =4.5 L/min, injection angle =75°, substrate temperature = 140℃, and injection distance =130mm*

Specimen No.	Arc current	Hardness Hv_3	Tensile bond strength (M.Pa)	Corrosion rate (mpy)	Porosity (%)	Thickness (μm)
$^{/}S_0$	750	700	45	$0.12 X10^{-3}$	2	220
$^{/}S_2$	850	685	44	$3 X10^{-3}$	4.5	200
$^{/}S_3$	450	660	43	$505 X10^{-3}$	13.7	110

Table (8): ***Show the effect of the injection angle on the coating performance at Ar-gas flow rate =65 L/min, H_2-gas flow rate =4.5 L/min, arc current =750A, substrate temperature =140℃, and injection distance =130mm***

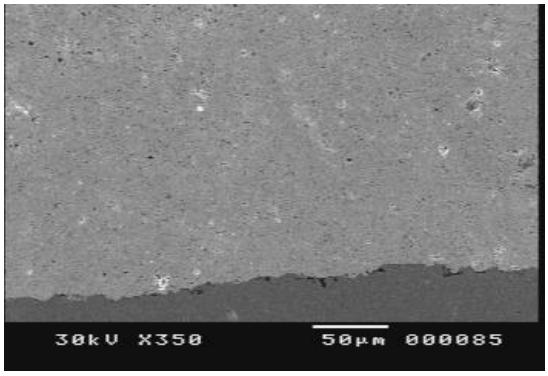
Specimen No.	Injection angle (degree)	Hardness (Hv_3)	Tensile bond strength (M.Pa)	Corrosion rate (m.p.y)	Porosity (%)	Thickness (μm)
$^{/}S_0$	75°	700	45	0.12 $X10^{-3}$	2	220
$^{/}S_2$	35°	675	43.3	53 $X10^{-3}$	8.5	190

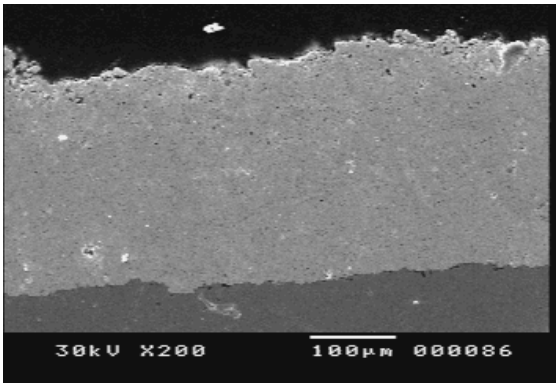
Table (9): ***Show the effect of the plasma gas on the coating performance at Ar-gas flow rate = 65 L/min, H_2-gas flow rate =4.5 L/min, injection angle =75°, substrate temperature = 140℃, and injection distance =130mm***

Specimen No.	Cooling air jet	Maximum substrate temperature (C°)	Hardness (HV_3)	Tensile bond strength (M.Pa)	Corrosion rate (mpy)	Porosity (%)	Thickness (μm)
$^{/}S_0$	Optimum placed	140	700	45	0.12 $X10^{-3}$	2	220
$^{/}S_5$	Wrongly placed	350	670	43	190 $X10^{-3}$	10	150

Table (10): ***Show the effect of injection distance on coating performance at Ar-gas flow rate =65 L/min, H_2-gas flow rate =4.5 L/min, arc current =750A, injection angle =75℃, and substrate temperature =140℃***

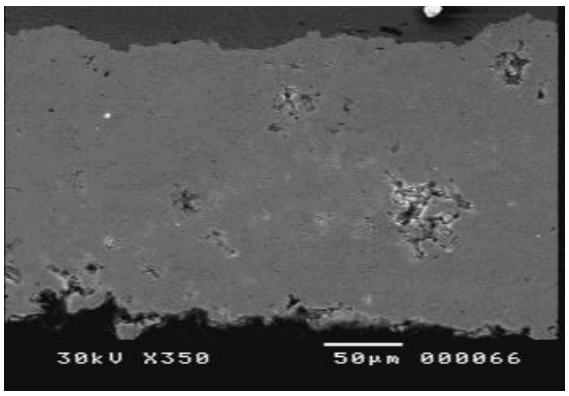
Specimen No.	Spraying distance (min)	Substrate temperature (°C)	Hardness (HV_3)	Tensile bond strength (M.Pa)	Corrosion rate (mpy)	Porosity (%)	Thickness (μm)
$^{/}S_0$	130	140	700	45	0.12 $X10^{-3}$	2	220
$^{/}S_6$	75	400	690	44.5	0.94 $X10^{-3}$	7.5	210
$^{/}S^7$	200	120	680	43.7	14 $X10^{-3}$	8.2	150

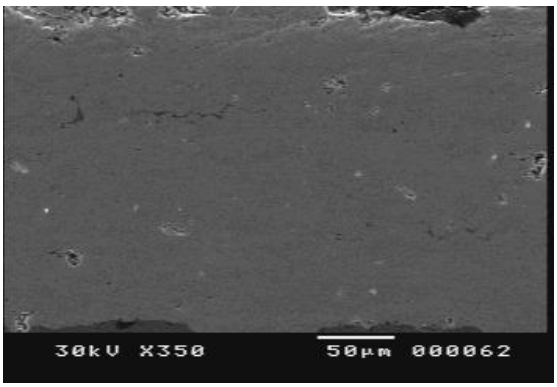




/S0 ***/S0***

Tungsten carbide coatings sprayed with the optimum conditions

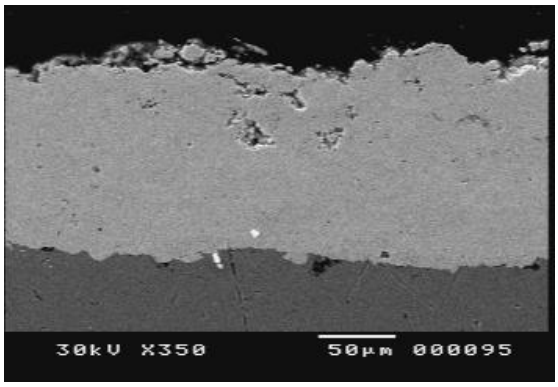


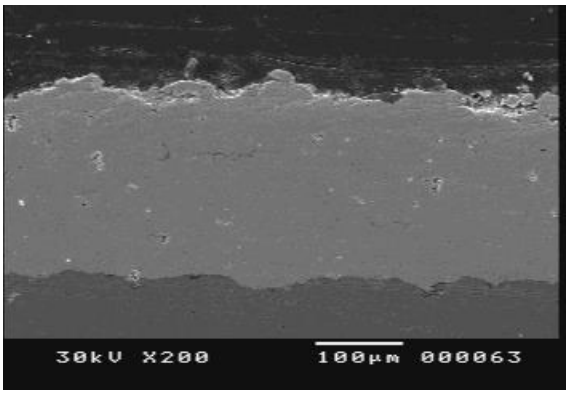


/S_1 ***/S_2***

Pure Ar (no H_2) arc voltae 50V, ***850A***

porosity percentage 4.5% ***prosity percentage 4.5***

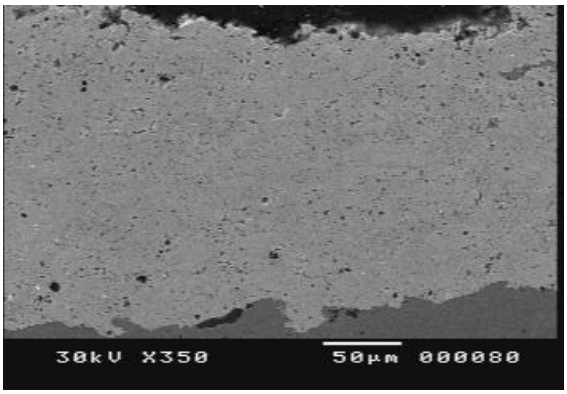




/S_3 ***/S_4***

450A ***Injection angle 35°***

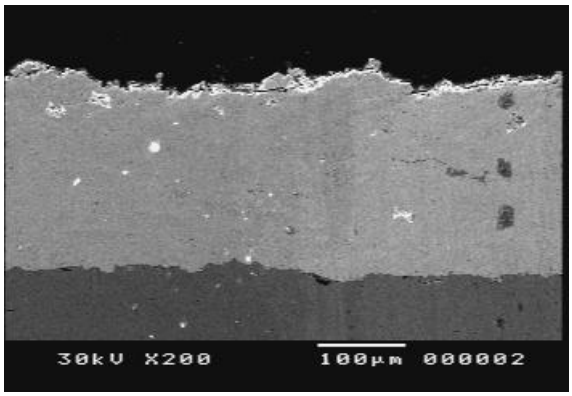
porosity percentage 13.7% ***Porosity percentage 8.5%***



$^{/}S_5$

Wrongly placed of applied cooling air jet

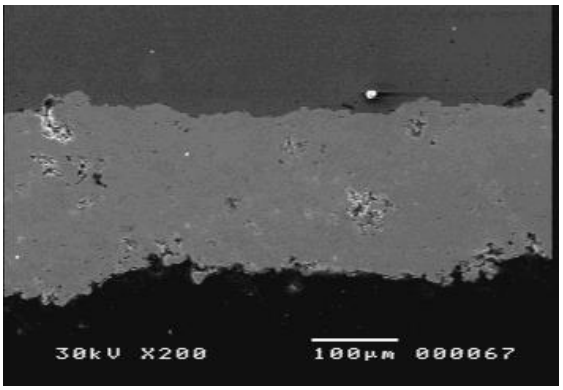
Porosity percentage 10%



$^{/}S_6$

Spraying distance 75mm, substrate temperature 400℃

Porosity percentage 7.5%



$^{/}S_7$

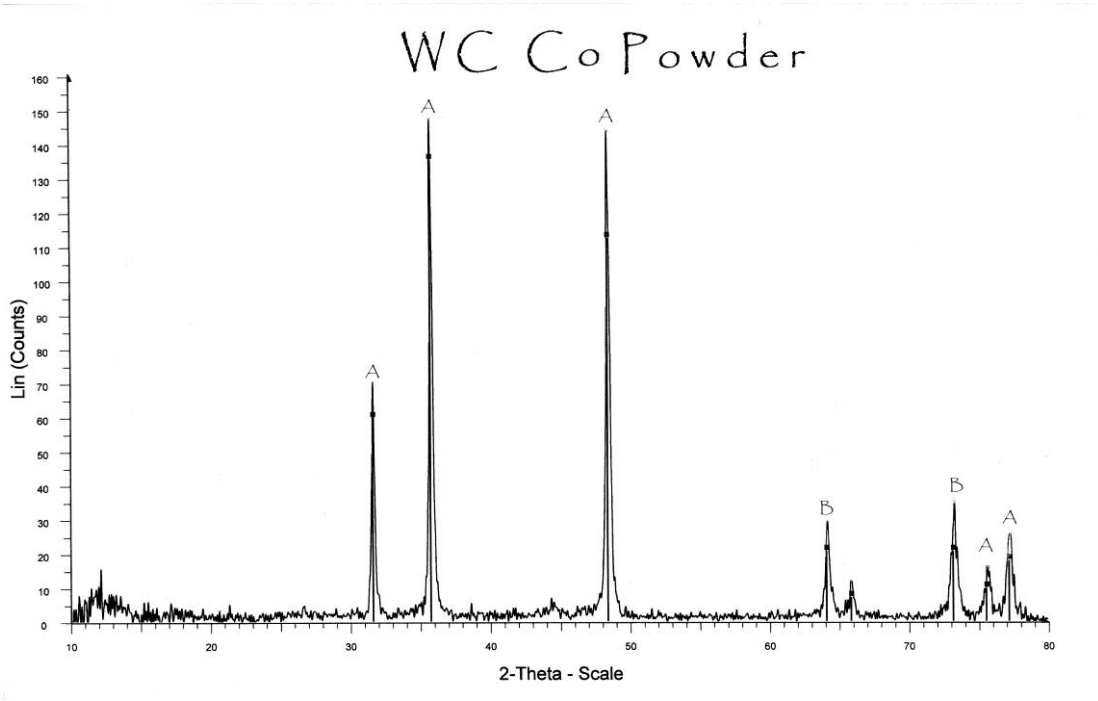
Spraying distance 200mm, substrate temperature 120℃,

porosity percentage 8.2%

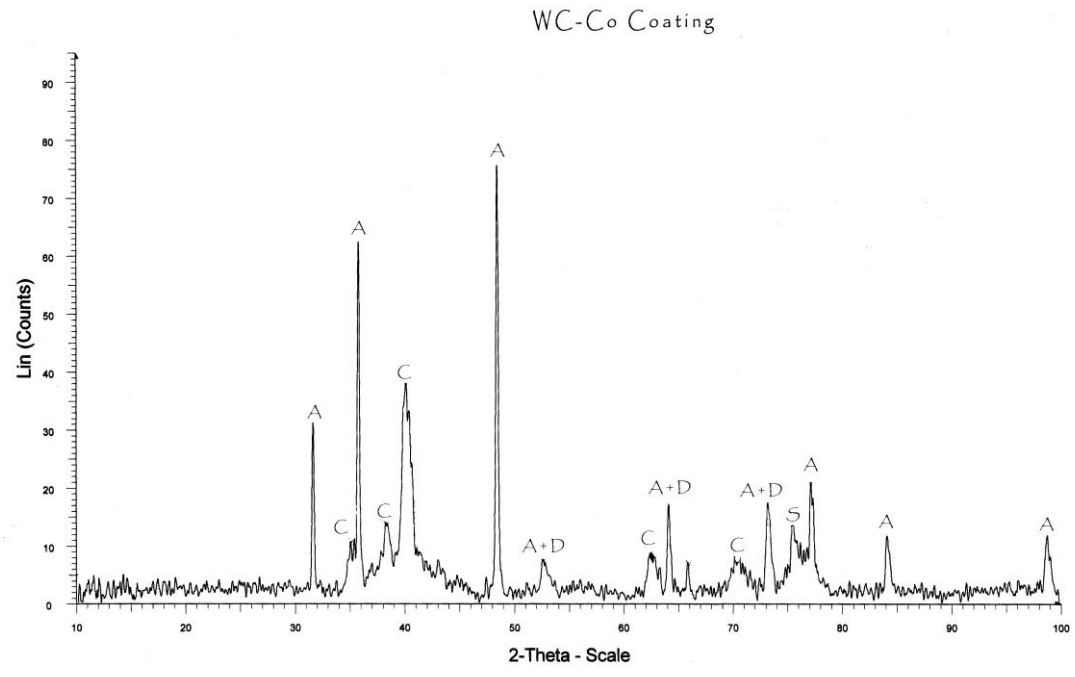
<u>Fig. (6):</u> Back scattered SEM image for cross section view of (WC-12wt% Co) coatings sprayed with the optimum conditions ($^{/}S_0$) with decreasing of the H_2-gas flow rate ($^{/}S_1$), with increasing of the arc current ($^{/}S_2$), with decreasing of the arc current t($^{/}S_2$), with decreasing of the injector angle ($^{/}S_4$), wrongly placed of the cooling air jet ($^{/}S_5$), with decreasing of the spraying distance ($^{/}S_6$) and with increasing of the spraying distance ($^{/}S_7$).

4.2 Powder Structure and Phase Composition.

Carbides are, together with oxides, the hardest thermally sprayed coatings, and the most often sprayed is tungsten carbide. The tungsten carbide containing 12% wt. of (Co) and average carbide grains of 5-10 μ m gives the greatest micro hardness after plasma spraying. X-ray analysis is-A comparison of X- ray diffraction results for the initial WC-Co spray powder and typical as – deposited coating in Figure (7) indicates that a substantial amount of WC phase was converted to W_2 C and W2 (C,O) during the plasma spray process. (a), a WC- 12 wt.% Co spray powder (b), and a baseline coating. The results for the as-deposited coating also show a broad elevated region or hump with extends roughly over 2 Ø values from 37 to 70 degrees. This indicates a poor degree of ordering and possibly amorphous or microcrystalline material in the as – deposited coating. It is noteworthy that amorphous, microcrystalline, and meta-stable phase due to the high cooling rate that are inherent in this process.



(a)



<u>Fig (7):</u> X- ray diffraction results of powder and coating

4.3 Tensile Boned Strength.

Carbides sprayed with the PLASMA-TECHNIK AG M-1000 apparatus have clearly lower adhesion strength (45 M.pa) than that, sprayed with HVOF and D- gun (greater than 50 M.pa). As the particle velocity is lower while using this technique, care must be taken in order to carefully optimize the plasma processing parameters (Table 3), in the way to obtain the most molten particles. Table (6-10) show the effect of changing coating parameters on tensile bond strength of different coatings obtained.

4.4 Hardness.

APS processing parameters have much less influence on the coating micro hardness, than parameters related the use powder. The hardness of WC-Co coating depends on amount, size and distribution of WC phase, amount and mean free path of the binder (Co). The temperature effect by using APS technique results in coatings of less hardness (HV_3 700) than D-gun and HVOF coatings. This is due to the decomposition of WC in hot oxidizing flame to W_2C following the reaction (84):

$$2WC \longrightarrow W_2C + C$$
$$W_2C + 0.5O_2 \longrightarrow W_2(C,O)$$
$$W_2(C, O) \longrightarrow 2WC + CO.$$

A comparison of hardness results for the tungsten carbide coatings of different spray conditions and the substrate (base) material can be illustrated in table (11).

Table (11): ***Show the hardness of substrate material and tungsten carbide coating with different spray conditions***

Specimen no.	Substrate material	Tungsten carbide coating material							
	S	$^{/}S_0$	$^{/}S_1$	$^{/}S_2$	$^{/}S_3$	$^{/}S_4$	$^{/}S_5$	$^{/}S_6$	$^{/}S_7$
Hardness HV_3	250	700	688	685	660	675	670	690	680

4.5 Corrosion Efficiency (%)

Table (12) show the electrochemical parameters derived from linear polarization on experiment for the tungsten carbide coatings of different spray conditions. The highest Corrosion protection amounts to 99.98% for specimen under the optimum condition, ($^{/}S_0$). However, the efficiency depends on applied tungsten carbide coating parameters.

Table (12): ***Results of linear polarization experiments.***

Specimen no.	E_{Corr} (V)	R_P (ohm.Cm^2 x 10^3)	I_{Corr} ($\mu A/Cm^2$)	Corrosion rate (m.p.y)	Efficiency (%)
S (blank) substrate	-0.297	8.416	3.2906	0.97832	—
$^{/}S_0$	-0.086	1.024×10^4	4.235×10^{-4}	0.12×10^{-3}	99.98
$^{/}S_1$	-0.165	2.899×10^3	1.678×10^{-2}	4×10^{-3}	99.5
$^{/}S_2$	-0.153	3.969×10^3	1.245×10^{-2}	3×10^{-3}	99.6
$^{/}S_3$	-0.315	4.993 x10	1.705	505×10^{-3}	48.3
$^{/}S_4$	-0.318	8.336 x10	1.802×10^{-1}	53×10^{-3}	94.5
$^{/}S_5$	-0.256	7.293 x10	6.455×10^{-1}	190×10^{-3}	80.5
$^{/}S_6$	-0.09	9.118×10^2	3.209×10^{-3}	0.94×10^{-3}	99.90
$^{/}S_7$	-0.065	5.66×10^2	4.89×10^{-3}	14×10^{-3}	98.5

5- Conclusion

In this study, APS of WC-12 wt.% Co was investigated using several systems to conclude the influence of plasma spray parameters on the coating performance, from the obtained data, discussion and interpretation of the results, it could be concluded that:

1- **The effect of hydrogen may be roughly explained: the hydrogen ionization potential is lower than Argon only by about 2 electron volts, and the high thermal conductivity of hydrogen at temperature higher than 400k results in a severe constriction of the arc column reducing the enhanced conductive thermal loses. These phenomena load to an increase of the electric field strength, and thus, of the arc voltage.**

2- **The hydrogen flow rate has no effect on the particle velocity. The reason is that the acceleration of particle is linked to the flow momentum, which means that it depends strongly on the mass flow rate of the plasma gas. Because Argon ions are much heavier than hydrogen ions. The mass flow rate of Argon was much higher than that of hydrogen. Correspondingly, Argon was mainly responsible for accelerating the powder particles. The higher particle velocity resulted in a worse melting behavior of the powder due to the shorter dwell time, leading to a lower coating thickness, namely a lower deposition efficiency of the powder.**

3- **The arc current play a very important role with the increase of the pumping effect led to an increase in the particle velocity as well as in the particle surface temperature. The decrease in the plasma powder led to a decrease in the deposition efficiency.**

4- **A change in color of the coating being sprayed indicates that the cooling jets are wrongly placed, the efficiency level of the spraying and the physical properties of the coating e.g. density, bond strength, and hardness. The pumping of the cooling air jets (which cools the Ar-H_2 plasma jet and the**

substrate) prevents the supper heating effect and deformation of the substrate because during spraying, heat could be transferred to the substrate from the plasma plume through two mechanisms during the solidification of the molten particles, the latent heat of solidification associated with the phase change from liquid to solid state will be released and conducted to the lower layers. After solidification, the newly solid layers continue to transfer heat due to high initial temperature (close to melting point) to lower temperature underlying layers and substrate.

5- **As the injection angle decreases (or as the injection distance increases), the droplet temperature decreases, the number of droplets which impact normally decreases because a deviation occurs for the droplet during flight for long distance; and the oxides appeared because the droplet dwell time is high enough to allow the droplets to react with the atmospheric oxygen.**

6- **It is difficult to achieve thermal spray coatings without causing some thermal decomposition (oxidation or decarburization of WC phase in the hot zone of the flame).**

7- **APS processing parameters have much less influence on the coating micro hardness, than the parameters related to the used powder.**

8- **It is noteworthy that amorphous microcrystalline, and metastable phase are commonly observed in plasma sprayed materials due to the high rate (rapid solidification and rapid cooling) that are inherent in this process.**

A substantial amount of the WC phase was converted to W_2C and W_2 (C, O) during the plasma spray process. The coating microstructure varied with coating thickness and extensive amount of WC phase is formed near the substrate because of the rapid solidification of flight particles.

9- **The electron dispersive x-ray (E.D.X) analysis of outer coating and inner coating (coating/ substrate interface) are not the same due to the diffusion of**

powder into the substrate material leading to increase of the tensile bond strength.

10- As the surface roughness increases, the tensile bond strength increases. The strengths are correlated with material used to spray, its size and method of preparation, processing technique, the selection of parameter, substrate thermo physical properties (e.g. thermal conductivity), and the state of its surface (roughness/ or the way of roughening). Ideally the substrate/ coating temperature during deposition should be high enough to promote good cohesion coating, but not so high that coating adhesion is seriously impaired.

11- The deviation of the spray parameters from the optimum condition lead to high corrosion rates with lower efficiencies.

12- The corrosion resistance properties of low-carbon steel alloys are enhanced significantly by thermal spray treatment.

13- The specimens which treated under the optimum conditions have the lowest corrosion rate and the thickest layer.

6-References

2 **R.L. Hao, Thermal Spraying Technology and Its Applications in the Iron & Steel Industry in China, *Thermal Spray 2007: Global Coating Solutions*, B.R. Marple, M.M. Hyland, Y.C. Lau, C.J. Li, R.S. Lima, and G. Montavon, Ed., 14-16 May, 2007 (Beijing, China), ASM International, Materials Park, OH, 2007, p 291-296.**

3 **Giacobbe, F.W., High Temperature Technology, 8(1), pp. 3-8 (1990).**

4 **F. Azarmi, M. Bashirzadeh, C. Leither, and G. Karami, Investigation on Relationship between Mechanical Properties and Microstructural Characteristics of Metal Matrix Composites Fabricated by Cold Spraying Technique, Proceedings of the International Meeting on Developments in Materials, Processes and Applications of Emerging Technologies, July 2-4, 2012, Alvor, Portugal.**

5 **F. Azarmi, V.J. Gelling, and M. Yan, Corrosion Behavior of Air Plasma Sprayed Alloy 625 on Nickel Foam Substrate, Proceedings of 2011 International Annual Corrosion Conference and Exposition (NACE), March 13-17, 2011 Houston, TX, USA.**

6 **T. Chandanayaka and F. Azarmi, Investigation on Microstructural and Mechanical Properties of Cold Sprayed & P/M Processed Ni-Ni_3Al Composites, ITSC 2013- Proceedings of the International Thermal Spray 2013, pp. 149-154, May 13-15, Busan, South Korea.**

7 **S. Yılmaz, Ceramics International 35, 2017 (2009).**

8 **F. Vargas, H. Ageorges, P. Fournier, P. Fauchais, M. E. Lopez, Surface and Coatings Technology 205, 1132 (2010).**

9 **S. T. Aruna, N. Balaji, J. Shedthi, V. K. W. Grips, Effect of critical plasma spray parameters on the microstructure, microhardness and wear and corrosion resistance of plasma sprayed alumina coatings, Surface & Coatings Technology 208 (2012)92–100.**

10 **N. Dejang, A. Watcharapasorn, et al.: Surface and Coatings Technology, Vol. 204(2010), p. 1651**

11 **Omidiji, B.V., Owolabi, H.A. and Khan, R.H. (2015) Application of Taguchi's Approach for Obtaining Mechanical Properties and Microstructures of Evaporative Pattern Castings. The International Journal of Advanced Manufacturing Technology, 79, 461-468. http://dx.doi.org/10.1007/s00170-015-6856-1**

12 **M. Moss, Dispersion Hardening in Al-V by Plasma Jet Spray Quenching, Acta Metall., vol. 16, 1968, p. 321-326.**

13 **Azarmi, F., Coyle, T., Mostaghimi, J. and Pershin, L. (2009) A New Approach to Develop High Temperature Foam Core Sandwich Structures Using Air Plasma Spraying. International Journal of Advanced Manufacturing Technology, 44, 900-905.**

14 **Bolleddu, V., Racherla, V. and Bandyopadhyay, P.P. (2014) Microstructural and Tribological Characterization of Air Plasma Sprayed Nanostructured Alumina-Titania Coatings Deposited with Nitrogen and Argon as Primary Plasma Gases. Materials & Design, 59, 252-263.**

15 **Pickard, J., Carretaro, J.A. and Bhavsar, V.C. (2016) On the Convergence and Origin Bias of the Teaching-Learning-Based-Optimization Algorithm. Applied Soft Computing, 46, 115-127.**

16 **Rao, R.V. (2016) Jaya: A Simple and New Optimization Algorithm for Solving Constrained and Unconstrained Optimization Problems. International Journal of Industrial Engineering Computations, 7, 19-34.**

17 **Maity, S.R. and Chakraborty, S. (2015) Tool Steel Material Selection Using PROMETHEE II Method. The International Journal of Advanced Manufacturing Technology, 78, 1537-1547.**

18 **Zhang, Y.W., Zou, P., Li, B.Z. and Liang, S. (2015) Study on Optimized Principles of Process Parameters for Environmentally Friendly Machining Austenitic Stainless Steel with High Efficiency and Little Energy Consumption. The International Journal of Advanced Manufacturing Technology, 79, 89-99. http://dx.doi.org/10.1007/s00170-014-6763-x**

19 **V.V. Sobolev, J.M. Guilemany, Influence of Droplet Impact Angle on Droplet-Substrate Mechanical Interaction in Thermal Spraying, Mater. Lett. 33, 1998, p. 315-319.**

20 **G. Montavon, S. Sampath, C.C. Berndt, H. Herman C. Coddet, Effects of Spray Angle on Splat Morphology during Thermal Spraying, Surface and Coat Technol., 91, 1997, p. 107-115.**

21 **P. Ctibor, P. Bohac, M. Stranyanek, R. Ctvrtlik, Structured and Mechanical Properties of Plasma Sprayed Coatings of Titania and Alumina, J. Eur. Ceram. Soc., 26, 2006, p. 3509-3514**

22 **X. Jiang, J. Matejicek, S. Sampath, Substrate Temperature Effects on Splat Formation, Microstructure, Development and Properties of Plasma Sprayed Coatings Part II: Case Study for Molybdneum, Mater. Sci. Eng. A272, 1999, p. 189-198.**

23 **A. Satapathy, S. P. Sahu, and D. Mishra, "Development of protective coatings using fly ash premixed with metal powder on Aluminium substrates," Waste Management and Research, vol. 28, no. 7, pp. 660–666, 2010.**

24 **T. Watanabe, I. Kuribayashi, T. Honda, and A. Kanzawa, Deformation and solidification of a droplet on a cold substrate, Chem. Eng. Sci., Vol. 47 (No. 12), 1992, p. 3059-3065.**

25 **C. San Marchi, H. Liu, E.J. Lavernia, R.H. Rangel, A. Sickinger, and E. Muehlberger, Numerical analysis of the deformation and solidification of a single droplet impinging onto a flat substrate, J. Mater. Sci., Vol. 28, 1993, p3313-21.**

26 **G. Gupta and A. Satapathy, "Modified mechanical and wear characteristics of epoxy filled with borosilicate glass micro-spheres," in Proceedings of the International Conference on Advancements in Polymeric Materials, CIPET, Lucknow, India, 2013.**

27 **V.V. Sobolev, J.M. Guilemany, and J.A. Calero, Substrate-coating thermal interaction during high velocity oxy-fuel (HVOF) spraying, part 1, Heat transfer processes, Mater. Sci. Technol., Vol. 11 (No. 8), 1995, p.810-819.**

28 **Fauchais, P., Fukomoto, M., Vardelle, A. and Vardelle, M., Knowledge Concerning Splat Formation: An Invited Review, Journal of Thermal Spray Technology, 13 (3), pp. 337 - 360, (2004).**

29 **Raessi, M., Mostaghimi, J. and Bussmann, M., "Droplet Impact during the Plasma Spray Coating Process-Effect of Surface Roughness on Splat Shapes," Proc. 17th Int. Symposium on Plasma Chemistry – ISPC 17, Toronto, Canada, (2005)**

30 **D. Landes, T.V. Streibel, J. Zierhut, (2002) Proceedings of ITSC 2002, Essen, Germany, 2002, pp. 45.**

31 **P. Bertrand, I. Smurov, M. Ignatiev, (2002) Proceedings of ITSC 2002, Essen, Germany, 2002, pp. 66.**

32 **Gómez J, Salazar A, Múnez C, Utrilla V and Poza P 2007 Bol. Soc. Esp. Ceram. 46 232**

33 **Ivosevic, M., Cairncross, R. A. and Knight, R., "Heating and Impact Modeling of HVOF Sprayed Polymer Particles," Proc. 2004 International Thermal Spray Conference (ITSC-2004), DVS/IIW/ASM-TSS, Osaka, Japan, (2004).**

34 **A. Ozturk and B.M. Cetegen, Modeling of Precipitate Formation in Precursor Droplets Injected Axially into an Oxygen/Acetylene Combustion Flame, *Mater. Sci. Eng.: A*, 2006, 422(1-2), p 163-175**

35 **G.E. Kim, Proven and Promising Applications Thermal Sprayed Nanostructured Coatings, PDF file in *Proceedings of the International Thermal Spray Conference 2006, PDF file in Building on 100 Years of Success: Proceedings of the International Thermal Spray Conference 2006*, B.R. Marple, M.M. Hyland, Y-C. Lau, R.S. Lima, and J. Voyer, Ed., May**

15-18, 2006 (Seattle, WA, USA), ASM International, Materials Park, OH, USA, 2006

36 **C. Delbos, J. Fazilleau, V. Rat, J.F. Coudert, P. Fauchais, B. Pateyron, Phenomena Involved in Suspension Plasma Spraying, Part 1: Suspension Injection and Behaviour, Plasma Chem. Plasma Process., 2006, 26(4), 371–391**

37 **R. Siegert, *A Novel Process for the Liquid Feedstock Plasma Spray of Ceramic Coatings with Nanostructural Features*, Juelich Press, Germany, 2006, Jül-4205**

38 **J.B. Nerz, A. Kushner, A. J. Rotolico, J. Therm. Spray Technol. 1 (2) (1992) 147.**

39 **Milewski, 1973, Vinoyo et al., 1985b, Rangaswamy and Herman, 1986**

40 **Kohal, R.J.; Bächle, M.; Att, W.; Chaar, S.; Altmann, B.; Renz, A.; Butz, F. Osteoblast and bone tissue response to surface modified zirconia and titanium implant materials. *Dent. Mater.* 2013, *29*, 763–776. David L. Poerschke, Jason S. Van Sluytman, Kimberly Wong, Carlos G. Levi, Acta Materialia 61 (2013) 6743-6755.**

41 **Roualdes, O.; Duclos, M.-E.; Gutknecht, D.; Frappart, L.; Chevalier, J.; Hartmann, D.J. *In vitro* and *in vivo* evaluation of an alumina-zirconia composite for arthroplasty applications. *Biomaterials* 2010, *31*, 2043–2054.**

42 **Elisa M. Zaleski, Charlotte Ensslen and Carlos G. Levi, Journal of the American Ceramic Society (submitted, December 2013).**

43 **J.Y. Jeong, J. Park, I. Henins, S.E. Babayan, V.J. Tu, G.S. Selwyn, G. Ding and R.F. Hicks, J. Phys. Chem.,2000, 8027 (2000)**

44 **Sarikaya, O. (2005) Materials and design, 26 (1), pp. 53-57.**

45 **S. Kitahara, Japan. J. of composite materials, 13, 37-44 (1987).**

46 **D.M. Lipkin, J.A. Krogstad, Y. Gao, C.A. Johnson, W.A. Nelson, and C.G. Levi, Journal of the American Ceramic Society, 96 [1] 290-298 (2013).**

47 **Lusty, P.J.; Tai, C.C.; Sew-Hoy, R.P.; Walter, W.L.; Walter, W.K.; Zicat, B.A. Third-generation alumina-on-alumina ceramic bearings in cementless total hip arthroplasty. *J. Bone Jt. Surg.* 2007, *89*, 2676–2683.**

48 **Q. Wang, Z.H. Chen, Z.X. Ding, Tribol. Int. 42 (7) (2009) 1046.**

49 **S.F. Wayne, S. Sarnpath, J. Therm. Spray Technol. 1 (4) (1992) 307.**

50 **Z. Yao, J. Stiglich, T.S. Sudarshan, Met. Powder Rep. 53 (2) (1998) 32.**

51 **.L. Jacobs, M.M. Hyland, M.D. Bonte, J. Therm. Spray Technol. 8 (1) (1999) 125.**

52 **L. Jacobs, M.M. Hyland, M. De Bonte, J. Therm. Spray Technol. 7 (2) (1998) 213.**

53 **] A. Verstak, V. Baranovski, in: B.R. Marple, M.M. Hyland, Y.-C. Lan, R.S. Lima, J. Voger (Eds.), AC-HVAF Sprayed Tungsten Carbide: Properties and Applications, Thermal Spray 2006: Building on 100 Years of Success, ASM International, Seattle, WA, May 15–18, 2006, (paper 11827).**

54 A. Verstak, V. Baranovski, Deposition of carbides by activated combustion HVAF spraying, thermal spray solutions: advances in technology and application, May 10–14, 2004 (Osaka, Japan), DVS — German Welding Society, 2004, p. 551
55 R.Q. Guo, C. Zhang, Q. Chen, Y. Yang, N. Li, L. Liu, Corros. Sci. 53 (7) (2011) 2351.
56 S.L. Liu, X.P. Zheng, G.Q. Geng, Wear 269 (5–6) (2010) 362.
57 S. Matthews, M. Hyland, B. James, J. Therm. Spray Technol. 13 (4) (2004) 526.
58 V.A.D. Souza, A. Neville, J. Therm. Spray Technol. 15 (1) (2006) 106.
59 Joan M. Perry, Anne Neville, Trevor Hodgkiess, J. Therm. Spray Technol. 11 (2002) 536.
60 M. Magnani, P.H. Suegama, N. Espallargas, S. Dosta, C.S. Fugivara, J.M. Guilemany, A.V. Benedetti, Surf. Coat. Technol. 202 (19) (2008) 4746.
61 H. Capel, P.H. Shipway, S.J. Harris, Wear 255 (2003) 917.
62 P.H. Shipway, L. Howell, Wear 258 (2005) 303.
63 Y. Ishikawa, J. Kawakita, S. Osawa, T. Itsukaichi, Y. Sakamoto, M. Takaya, S. Kuroda, J. Therm. Spray Technol. 14 (3) (2005) 384.
64 Q. Wang, L.X. Li, G.B. Yang, X.Q. Zhao, Z.X. Ding, Surf. Coat. Technol. 206 (19–20) (2012) 4000.
65 D.A. Stewart, P.H. Shipway, D.G. Mccartney, Acta Mater. 48 (7) (2000) 1593.
66] M.S.A. Khan, T.W. Clyne, in: C.C. Berndt (Ed.), Thermal Spray: Practical Solutions for Engineering Problems, ASM International, Materials Park, Ohio, 1996, p. 113.
67 P. Aroto, L. Bartha, R. Porat, S. Berger, A. Rosen, Nanostruct. Mater. 10 (1998) 245.
68 B.H. Kear, G. Skandan, R.K. Sadangi, Scr. Mater. 44 (8–9) (2001) 1703.
69 J.R. Fincke, W.D. Swank, D.C. Haggard, Proceedings of the 7th National Thermal Spray Conference, ASM Int, Boston, 1994, p. 325.
70 C. Verdon, A. Karimi, J.L. Martin, Mater. Sci. Eng., A 246 (1–2) (1998) 11.
71 D. Zhang, S.J. Harris, D.G. McCartney, Mater. Sci. Eng., A 344 (1–2) (2003) 45.
72 P. Chivavibul, M. Watanabe, S. Kuroda, K. Shinoda, Surf. Coat. Technol. 202 (3) (2007) 509.
73 Q. Yang, T. Senda, A. Ohmori, Wear 254 (1–2) (2003) 23.
74 S.H. Zhang, T.Y. Cho, J.Ho. Yoon, M.X. Li, P.W. Shum, S.C. Kwon, Mater. Sci. Eng. B 162 (2) (2003) 127.
75 C. Monticelli, A. Frignani, F. Zucchi, Corros. Sci. 46 (5) (2004) 1225.
76 A. Trueman, D.P. Schweinsberg, G.A. Hope, Corros. Sci. 41 (7) (1999) 1377.
77 M. Takeda, N. Morihiro, R. Ebara, Y. Harada, Mater. Trans. 43 (11) (2002) 2860.
78 G. Bolelli, R. Giovanardi, L. Lusvarghi, T. Manfredini, Corros. Sci. 48 (11) (2006) 3375.
79 P.H. Suegama, C.S. Fugivara, A.V. Benedetti, J. Fernández, J. Delgado, J.M. Guilemany, Corros. Sci. 47 (3) (2005) 605.